Hydrophobic and Electrostatic Interactions between Adrenocorticotropin-(1–24)-tetracosapeptide and Lipid Vesicles. Amphiphilic Primary Structures†

Beat Gysin and Robert Schwyzer*

ABSTRACT: Hydrophobic photolabeling with 3-(trifluoromethyl)-3-(*m*-[^{125}I]iodophenyl)diazirine ([^{125}I]TID [Brunner, J., & Semenza, G. (1981) *Biochemistry 20*, 7174–7182]) and equilibrium dialysis were used to study hydrophobic and electrostatic interactions between three adrenocorticotropin fragments and liposomes prepared from mixtures of phosphatidylcholine with phosphatidic acid or phosphatidylserine. Corticotropin-(1–10)-decapeptide ($ACTH_{1-10}$, net charge 0) formed hydrophobic clusters with [^{125}I]TID in aqueous solutions at peptide concentrations above 1 μM but did not interact appreciably with neutral or anionic liposomes. Corticotropin-(11–24)-tetradecapeptide ($ACTH_{11-24}$, net charge 6+) reacted electrostatically with anionic liposomes but showed no hydrophobic interactions. Corticotropin-(1–24)-tetracosapeptide ($ACTH_{1-24}$, net charge 6+), a covalent combination of the two fragments, exhibited both hydrophobic and electrostatic interactions with lipid vesicles. Edman degradation and chymotryptic hydrolysis of labeled $ACTH_{1-24}$ revealed that the hydrophobic interaction involved the N-terminal decapeptide "message" segment (corresponding to $ACTH_{1-10}$) which entered the membrane and that the electrostatic interaction was caused by the C-terminal tetradecapeptide "address" segment (corresponding to $ACTH_{11-24}$) which remained on the aqueous membrane surface. This behavior is in complete analogy to that reported for dynorphin-(1–13)-tridecapeptide by Gysin and Schwyzer [Gysin, B., & Schwyzer, R. (1983) *FEBS Lett. 158*, 12–16; Gysin, B., & Schwyzer, R. (1983) *Arch. Biochem. Biophys. 225*, 467–474]: in both cases, the specific, hydrophobic membrane interaction of the "message" critically depended on the presence of the hydrophilic "address". The results reported here were consistent with those obtained by infrared attenuated total reflection spectroscopy [Gremlich, H.-U., Fringeli, U.-P., & Schwyzer, R. (1983) *Biochemistry 22*, 4257–4263] and were crucial for their interpretation. Thus, $ACTH_{1-24}$ is adsorbed to neutral multibilayer membranes. Its polycationic C-terminal tetradecapeptide remains on the membrane surface, assuming an extended conformation with peptide bond transition dipoles oriented perpendicularly to the membrane surface. The quite hydrophobic N-terminal decapeptide assumes a helical conformation in the membrane with the axis oriented perpendicularly to the bilayer plane. Our model provides novel correlations between peptide structure, membrane interactions, and pharmacological properties. It is an example of the importance of peptide amphiphilicity as a cause for membrane interactions. In our case, the amphiphilicity is due to the segmental ("sychnologic") organization of the primary structure and not to the secondary folding of a "rhegnylogically" organized chain to produce amphiphilic secondary structures, such as amphiphilic helixes or β-pleated sheets.

Adrenocorticotropin-(1–24)-tetracosapeptide ($ACTH_{1-24}$),[1] (+)Ser-Tyr-Ser-Met-Glu(−)-His-Phe-Arg(+)-Trp-Gly-Lys-(+)-Pro-Val-Gly-Lys(+)-Lys(+)-Arg(+)-Arg(+)-Pro-Val-Lys(+)-Val-Tyr-Pro(−), net charge 6+, is a potent full agonist for all known biological actions of the natural hormone $ACTH_{1-39}$ [for a review, see Schwyzer (1977)]. It elicits its effects by reacting with specific receptors located in the outer membrane of its target cells (Schulster & Schwyzer, 1980). The lipid phase of the membranes acts as a matrix for the receptors and is essential for the functionality and the topological deployment of the receptor proteins [see Sonenberg & Schneider (1977)]. Is the lipid phase also responsible for the proper function of $ACTH_{1-24}$, perhaps by serving as an antenna to capture the peptide from the intercellular space, as suggested on theoretical grounds by Adam & Delbrück (1968) and by Berg & Purcell (1977), or by inducing topological arrangements and secondary structures of the peptide that would facilitate rapid and correct receptor contacts (Schwyzer, 1963, 1977)?

We studied this question with three methods using artificial membranes prepared from pure lipids [preliminary account: Schwyzer et al. (1983)]. Capacitance minimization (Gremlich et al., 1981), infrared attenuated total reflection spectroscopy (IR-ATR; Gremlich et al., 1983), and vesicle-mediated hydrophobic photolabeling (the subject of this report) have led to a rather detailed model for the interaction of $ACTH_{1-24}$ with lipid membranes. Thus, $ACTH_{1-24}$ is adsorbed from aqueous solutions onto planar dioleoylphosphatidylcholine membranes strongly enough to satisfy the requirements set forth by Berg & Purcell (1977) for peptide capture and reduction of dimensionality in the process of receptor search. The hydrophilic, C-terminal tetradecapeptide segment assumes an extended, random conformation on the membrane surface with perpendicularly oriented planes of the peptide bonds. The more hydrophobic N-terminal decapeptide segment enters the membrane as a helical structure with the helix axis perpendicular to the membrane surface.

In this report we describe in detail the contribution of vesicle-mediated hydrophobic photolabeling with the reagent of Brunner & Semenza (1981), 3-(trifluoromethyl)-3-(*m*-[^{125}I]iodophenyl)diazirine, [^{125}I]TID, and of experiments with equilibrium dialysis to our understanding of hydrophobic and electrostatic interactions between ACTH peptides and neutral or anionic liposomes. The observed interactions correlate well

† From the Department of Molecular Biology and Biophysics, Swiss Federal Institute of Technology (ETH), CH-8093 Zürich, Switzerland. *Received July 25, 1983.* Supported by project grants of the ETH, the Swiss National Science Foundation, and the Bonizzi-Theler Stiftung.

[1] Abbreviations: ACTH, adrenocorticotropic hormone; $ACTH_{n-m}$, synthetic ACTH peptides comprising the amino acid residues *n* to *m* of the natural (human) sequence; PC, phosphatidylcholine (egg yolk lecithin); PA, phosphatidic acid (dipalmitoyl); PS, phosphatidylserine (brain); TID, 3-(trifluoromethyl)-3-(*m*-iodophenyl)diazirine.

0006-2960/84/0423-1811$01.50/0

with pharmacological properties and appear to be biologically relevant (Gysin & Schwyzer, 1983a). The essential features, the N-terminal, pharmacologically defined "message" segment (Schwyzer, 1977) entering the hydrophobic membrane layers and the C-terminal, potentiating "address" segment lying on the membrane surface, apply also to the extremely potent opioid peptide, dynorphin (Gysin & Schwyzer, 1983b).

In both cases, peptide hydrophobicity alone was insufficient to warrant membrane interaction of the message segments, but peptide amphiphilicity (presence of the address) was required. This amphiphilicity arose from the segmental distribution of hydrophobic and hydrophilic residues in the primary structure and corresponded with the segmental, "sychnologic" organization of pharmacological information as defined by Schwyzer (1977). The condition of amphiphilicity extends the list of molecular parameters that have to be considered in establishing quantitative structure–activity relationships.

The primary amphiphilicity described here contrasts in its origin to the secondary amphiphilicity caused by secondary folding of the peptide chain [amphiphilic α- and π-helixes (Kaiser & Kézdy, 1983) and amphiphilic β-structures]. Secondary amphiphilicity implies a "rhegnylogic" distribution of pharmacological information (Schwyzer, 1977). Primary and secondary amphiphilicity both appear to be important features of peptides depending on hydrophobic membrane interactions for their biological activity.

Experimental Procedures

Peptides. $ACTH_{1-10}$, $ACTH_{1-24}$, and $ACTH_{11-24}$ were prepared by the procedure of Schwyzer & Kappeler (1963).

Photolabel. 3-(Trifluoromethyl)-3-(*m*-[^{125}I]iodophenyl)-diazirine, [^{125}I]TID, was synthesized as described by Brunner & Semenza (1981) and had a specific activity of 3.7×10^{11} Bq/mmol.

Vesicles or liposomes from phosphatidylcholine (PC) or from mixtures of phosphatidylcholine with other lipids, e.g., PC–PA (molar ratio of 9:1), were prepared according to Enoch & Strittmatter (1979) using egg yolk lecithin (Singleton et al., 1965) and dipalmitoylphosphatidic acid (Lipid Products, Nutfield, NJ) in phosphate buffer A (10 mM phosphate, 100 mM NaCl, 0.1 mM EDTA, pH 7.3). The oxidation index determined spectroscopically (Klein, 1970) was less than 0.1. The lipid concentration was estimated as described by Raheja et al. (1973). Dr. M. Müller (Zürich, ETHZ) controlled the preparations by electron microscopy, using negative staining, freeze etching, and freeze substitution techniques (Müller et al., 1980; Meister & Müller, 1980) and found them to consist mainly of bilayer and some multibilayer vesicles with diameters between 50 and 200 nm.

Labeling. To 1 mL of a vesicle suspension in buffer A containing 1.5 mL of lipid, 10 μL of a 1 mM peptide solution and (3–8) $\times 10^5$ Bq of [^{125}I]TID were added. The solutions were thus about 10 μM in peptide, 1–2 μM in [^{125}I]TID, and about 2 mM in lipid. After incubation at 23 °C for 10 min, the samples were screened by a $CuSO_4$ filter (cutoff at 315 nm) and illuminated for 1 min with a 150-W mercury arc lamp that produced 1.5 W at the target, thus ensuring complete photolysis of the TID (Brunner & Semenza, 1981). Control experiments were carried out by omitting either the peptide, the label, or the liposomes. In other experiments, the concentrations of peptide and label were varied, and the pH was changed from 7.3 to 3 or 11.

Isolation of the Labeled Peptides. After disruption of the vesicles with 0.05 mL of Triton X-100 and adjustment of the pH to 4.5, the samples were applied to a column (0.5 × 5 cm) of carboxymethylcellulose (Whatman CM-52) that had been equilibrated with 0.01 N ammonium acetate, pH 4.5. After the column was washed with 300 mL of the same buffer in order to remove photoproducts and other material of nonpeptide nature, the labeled and unlabeled peptides were eluted with 1 M ammonium acetate, pH 7, as one sharp peak (0.5-mL fractions, flow rate 12 mL/h). Columns and elution volumes were routinely checked with 100 μL of a 1 mM aqueous solution of the peptide and monitored by the absorption at 280 nm. The absorption profiles coincided with the radioactivity profiles.

Labeling Rates. The chromatographic fractions were monitored by γ-counting (MR 480 γ-counter, W + W Electronics). The mean radioactivity in cpm of the peptide peak fractions of two to five independent labeling experiments, after subtraction of the blank values obtained from controls without peptide, was regarded as the "labeling rate".

Chymotryptic Digestion of Labeled $ACTH_{1-24}$. The labeled $ACTH_{1-24}$ (between 5000 and 10000 cpm) obtained from the peak fractions of the carboxymethylcellulose chromatogram (Figure 2) by lyophilization was dissolved in 1 mL of a 1 mM solution of unlabeled $ACTH_{1-24}$ in sodium bicarbonate (10 mM, pH 8). After addition of 1 mol % of chymotrypsin (Sigma), the solution was kept at about 20 °C for 15 h. The solution was lyophilized, adjusted to pH 4.5, and chromatographed through a carboxymethylcellulose column (1 × 9 cm) that had been equilibrated with 0.1 N ammonium acetate, pH 4.5. After having collected 22 fractions of 1 mL each at a flow rate of 25 mL/h, a linear gradient was applied that reached 1.0 M ammonium acetate, pH 7, during 60 further fractions. The chromatograms were monitored by γ-counting and eluate absorbance at 280 nm.

Edman Degradation. About 2000–3000 cpm of labeled $ACTH_{1-24}$ obtained from the peak fractions of the chromatographic separation (Figure 2) were degraded in a Beckman 890C spin cup sequenator (courtesy of Drs. G. Frank and H. Zuber, this department) by using a mixture of 3 mg of Polybrene and 150 nmol of β-lactoglobulin in 0.25 mL of Quadrol, according to the method of Tarr et al. (1978). Before use, the labeled material was 3 times lyophilized from distilled water to remove traces of ammonium acetate. During the first two steps, benzene extraction only was used in order to remove unspecifically bound label. The radioactivity of each step was measured directly, and the phenylthiohydantoins arising from the β-lactoglobulin were identified by high-pressure liquid chromatography (Frank & Zuber, 1976).

Polyacrylamide Gel Electrophoresis. The labeled peptides from the peak fractions were further characterized by polyacrylamide gel electrophoresis in the presence of sodium dodecyl sulfate (Reisfeld et al., 1962). After 3–4 h at pH 3.0, 175 V, and 4 mA/gel, the gels were cut into slices 4.5 mm thick. The radioactivity profile determined by γ-counting was compared with the fluorescence profile obtained by electrophoresis of a randomly dansylated sample, prepared from 5 nmol of unlabeled peptide according to Kato & Sasaki (1975).

Solubilization of [^{125}I]TID in Aqueous Peptide Solutions. [^{125}I]TID (0.5×10^6 cpm, dissolved in 1 μL of ethanol) was added to 10^{-9}–10^{-3} M solutions (0.5 mL) of the peptide in buffer A at pH 3 and 11. After the mixture was shaken and incubated for 15 min at 23 °C, the suspension was centrifuged and the radioactivity determined in a 75-μL aliquot of the clear supernatant.

Equilibrium Dialysis. $ACTH_{1-24}$ was labeled with ^{125}I according to the procedure of Eberle & Hübscher (1979) for α-MSH. However, the molar ratio of ^{125}I to peptide was

Table I: Hydrophobic Labeling of ACTH Peptides with [^{125}I]TID in the Presence and Absence of Phosphatidylcholine-Phosphatidic Acid (9:1) Vesicles[a]

peptide		peptide molarity	labeling rate (cpm) vesicle absence	labeling rate (cpm) vesicle presence[b]	rate ratio, presence: absence
$ACTH_{1-10}$[c]	(+)SYSME(–)HFR(+)WG(–)	10^{-5}	17400	3000	0.17
		10^{-4}	80000	18000	0.23
		10^{-3}	100000	12000[d]	0.12
$ACTH_{1-24}$	(+)SYSME(–)HFR(+)WGK(+)PVGK(+)K(+)R(+)R(+)P(+)VK(+)VYP(–)	10^{-5}	3700	10000	2.7
$ACTH_{11-24}$	(+)K(+)PVGK(+)K(+)R(+)R(+)PVK(+)VYP(–)	10^{-5}	2800	2700	1

[a] Typical experiments with (20–30) × 10^6 cpm/mL, or about 1 μM [^{125}I]TID; pH 7.3. [b] About 2 mM lipid. [c] Examined at pH 11 because of limited solubility; similar results were obtained at pH 3. [d] Presence of 10 mM sodium dodecyl sulfate instead of lipid vesicles; critical micelle-forming concentration of SDS about 8 mM.

reduced to 1:10 in order to suppress the formation of diiodinated $ACTH_{1-24}$ (Rae & Schimmer, 1974). Furthermore, albumin was omitted from the reaction, thus making the purification step with Sephadex LH-20 superfluous. Chromatography over Sephadex G-25 and carboxymethylcellulose CM-52 resulted in one peptide peak containing 93% of the total bound radioactivity. The specific activity was 1.4 × 10^{11} Bq/mmol.

Dialysis was carried out in dialysis cells in which two compartments of 1 mL each were separated by a membrane permeable for molecules of up to a molecular weight of 12000–14000. Into one compartment, 0.5 mL of the standard vesicle preparation, PC–PA (9:1) (1.5 mg of lipid/mL), was filled and, into the other, 0.5 mL of the peptide solution. The peptide solutions were prepared in phosphate buffer A and represented a series of concentrations of unlabeled $ACTH_{1-24}$, each solution containing, in addition, 20000 cpm of the preparation of ^{125}I-iodinated $ACTH_{1-24}$ described above.

After dialysis for 20 h at 23 °C, aliquots of 0.1 mL of each compartment were counted in the γ-counter for 10 min, and the difference was calculated. A difference of about 1 μmol/0.5 mL was at the detection limit. The results were the means and standard deviations derived from two probes each taken from two independent experiments.

Dialysis was also carried out in the presence of 1 mM $ACTH_{11-24}$ or with neutral vesicles, prepared from egg yolk lecithin alone.

Results and Discussion

(1) Solubilization of [^{125}I]TID in Aqueous Solutions of $ACTH_{1-10}$ and $ACTH_{1-24}$. $ACTH_{1-24}$ and $ACTH_{1-10}$ were investigated at pH 7.3, and $ACTH_{1-10}$ was investigated additionally at pH 3 and 11, because of its limited solubility at neutral pH above about 50 μM. As shown in Figure 1, $ACTH_{1-24}$ did not enhance the solubility of [^{125}I]TID in the range of concentrations tested. However, [^{125}I]TID was markedly solubilized in solutions of $ACTH_{1-10}$ above about 1 μM. At 10 μM $ACTH_{1-10}$, 1 molecule of [^{125}I]TID was solubilized by about 35000 molecules of $ACTH_{1-10}$.

The solubilizing effect of $ACTH_{1-10}$ was explained by the formation of hydrophobic aggregates with [^{125}I]TID above a critical peptide concentration of about 1 μM. This behavior was consistent with the predominantly hydrophobic nature of the amino acid side chains and the tendency of $ACTH_{1-10}$ to form antiparallel pleated sheet clusters (Gremlich et al., 1983).

$ACTH_{1-24}$ did not appear to aggregate with [^{125}I]TID at peptide concentrations between 1 nM and 1 mM. This behavior was consistent with the strong electrostatic repulsion expected for highly charged (6+) molecules of such size and amino acid composition.

(2) Hydrophobic Labeling of $ACTH_{1-10}$. In order to distinguish between vesicle-mediated and peptide aggregate

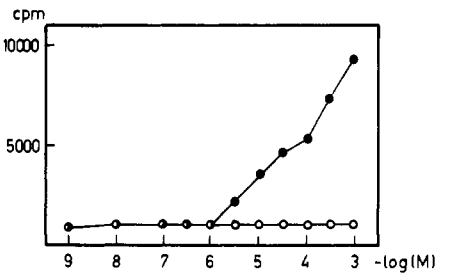

FIGURE 1: Solubilization of [^{125}I]TID as a function of peptide concentration. (Abscissa) Negative decadic logarithm of peptide molarity. (Ordinate) Solubilized radioactivity (cpm per 75 μL). (○) $ACTH_{1-24}$; (●) $ACTH_{1-10}$ at pH 3. The behavior of $ACTH_{1-10}$ at pH 11 was practically the same as that at pH 3. At pH 7.3, the results were the same up to the limit of solubility, which was between 50 and 100 μM.

mediated hydrophobic labeling, labeling rates were determined in the presence and in the absence of liposomes. In all experiments, a peak of radioactivity, coincident with the absorbance peak produced by unlabeled $ACTH_{1-10}$, appeared in the chromatograms immediately after raising the pH and the ionic strength of the eluant. This peak was absent in the control experiments without peptide (Figure 2). In terms of absolute labeling rates, the results were reproducible to about ±10% if the same preparation of [^{125}I]TID was used; for different photolabel preparations with different specific activities, the relative labeling rates with and without liposomes proved to be equally reproducible.

Table I shows that the labeling rate of the free peptide was concentration dependent. This was explained by the increased solubilization of [^{125}I]TID at $ACTH_{1-10}$ concentrations above 1 μM (Figure 1). At 10 μM peptide about 1 in every 15000 $ACTH_{1-10}$ molecules was labeled. This molar labeling ratio was of the same order of magnitude as the solubilization ratio (1:35000). The 2-fold difference was probably due to the excess of finely dispersed, insoluble [^{125}I]TID present in the labeling experiments but removed from the solubilization experiments.

The rate of labeling was reduced to about 20% or less in the presence of vesicles or of sodium dodecyl sulfate (Table I). The simplest explanation for this behavior was that the [^{125}I]TID present in the reaction mixture partitioned into the added lipid or tensid phases and became less available to the peptide. Such a dilution effect would only have been operative if it was not compensated by equally important hydrophobic interactions between $ACTH_{1-10}$ and the vesicles or micelles.

We thus concluded that hydrophobic labeling of $ACTH_{1-10}$ occurred predominantly from within mixed aggregates of the peptide and the photolabel but that $ACTH_{1-10}$ interacted only very weakly with PC–PA (9:1) vesicles in aqueous surroundings. This behavior was consistent with the results obtained

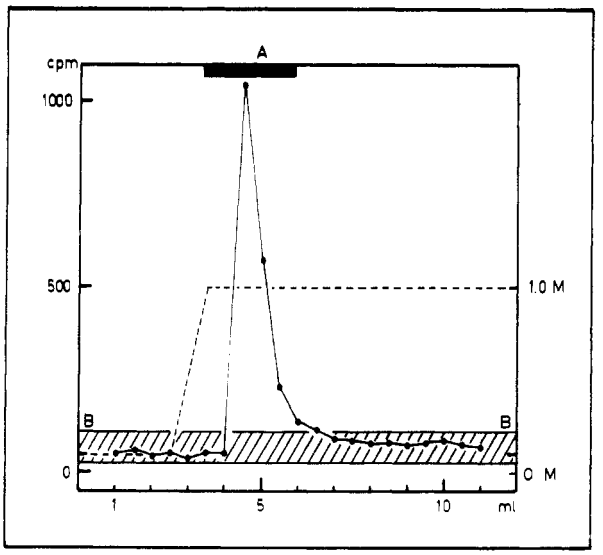

FIGURE 2: Carboxymethylcellulose chromatography of labeled $ACTH_{1-24}$. Results of an experiment in the presence of PC–PA (9:1) vesicles in which 5-fold amounts of all ingredients described under Experimental Procedures were applied. The chromatogram (column 0.5 × 5 cm) was washed with 300 mL of NH_4OAc, 0.1 M, pH 4.5, and then, at point 0 mL, the eluant was changed to 1.0 M NH_4OAc, pH 7. (Abscissa) Eluant volume (0.5-mL fractions). (Ordinate) Radioactivity (cpm per 0.5 mL). (A) Elution volume of unlabeled $ACTH_{1-24}$, $ACTH_{11-24}$, and $ACTH_{1-10}$. (B) Bandwidth of radioactive background in experiments without peptides. Chromatograms with labeled $ACTH_{11-24}$ and $ACTH_{1-10}$ presented qualitatively similar pictures, with quantitative differences mainly in the peak region.

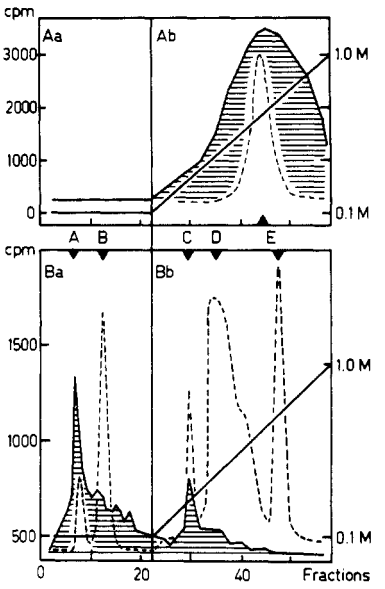

FIGURE 3: Carboxymethylcellulose chromatography of a mixture of [^{125}I]TID-labeled $ACTH_{1-24}$ before (panel A) and after (panel B) chymotryptic hydrolysis. In panels Aa and Ba, the eluant was 0.1 M NH_4OAc, pH 4.5; in panels Ab and Bb, an ionic strength and pH gradient were applied, reaching 1.0 M and pH 7.0. The dashed lines indicate absorbance at 280 nm and the shaded areas radioactivity above background (about 200–300 cpm, panel Aa). The absorbance peaks were correlated to peptides as follows (Shepherd et al., 1956): A, SMEHF (net charge 1– at pH 7); B, SY (0); C, RW (1+)); D, GKPVGK (2+, no contribution to the absorbance), KRRPVKVYP (4+), GKPVGKKRRPVKVYP (6+); E (in panels Ab and Bb), undegraded control $ACTH_{1-24}$ (6+).

by IR-ATR spectroscopy (Gremlich et al., 1983; Schwyzer et al., 1983).

(*3*) *Hydrophobic Labeling of $ACTH_{11-24}$.* As shown in Table I, the labeling rate was low both in the absence and in the presence of PC–PA (9:1) vesicles. Thus, $ACTH_{11-24}$ formed no mixed aggregates with [^{125}I]TID, which was not astonishing in view of its excess positive charge (6+ per molecule), although it contains quite a number of hydrophobic amino acid side chains (three valines, one tyrosine, and two prolines). It exhibited no vesicle-mediated labeling, although its electrostatic interaction with the negatively charged vesicles was shown to be quite strong (see section 9). This behavior was consistent with the conclusions drawn from the Edman and chymotryptic degradations of labeled $ACTH_{1-24}$ and supported the view that the C-terminal tetradecapeptide segment of $ACTH_{1-24}$ remained out of reach of [^{125}I]TID (in the aqueous phase or in the hydrophilic head group layer) upon interaction or collision with the lipid vesicles.

(*4*) *Hydrophobic Labeling of $ACTH_{1-24}$.* Typical results are shown in Figure 2 and in Table I. The cationic, radioactive material emerging from the carboxymethylcellulose column just after raising the ionic strength and the pH of the eluant undoubtedly contained [^{125}I]TID-labeled $ACTH_{1-24}$ as a main component. This was indicated by three observations: (i) the lack of the peak in control experiments without the peptide; (ii) the approximate identity of its electrophoretic mobility with that of a randomly, weakly dansylated sample of $ACTH_{1-24}$; (iii) its hydrolysis by chymotrypsin into smaller fragments with the expected properties and its degradation by the Edman procedure (see sections 5 and 6).

As expected from its inability to solubilize [^{125}I]TID, $ACTH_{1-24}$ was much less labeled in the absence of lipid vesicles than $ACTH_{1-10}$ (Table I). Its labeling rate was significantly enhanced in the presence of PC–PA (9:1) vesicles. This behavior indicated that, in contrast to $ACTH_{1-10}$, $ACTH_{1-24}$ formed no aggregates with [^{125}I]TID but, in the presence of liposomes, was brought into contact with the photolabel dissolved in the lipid membranes. We concluded that hydrophobic labeling of $ACTH_{1-24}$ with [^{125}I]TID in the presence of liposomes was predominantly mediated by the vesicles (for exclusion of another possible explanation, see section 8).

(*5*) *Chymotryptic Hydrolysis of Labeled $ACTH_{1-24}$.* In order to determine which parts of the peptide chain were labeled by [^{125}I]TID in the presence of PC–PA (9:1) vesicles, mixtures of labeled and unlabeled $ACTH_{1-24}$ were hydrolyzed by chymotrypsin. The hydrolysate was investigated by carboxymethylcellulose chromatography, using an ionic strength/pH gradient of ammonium acetate. The optical density indicated the position of unlabeled peptides, the radioactivity that of labeled peptides. Structures were assigned to the unlabeled peptides according to their relative elution volumes (Shepherd et al., 1956; Figure 3).

Before hydrolysis, all of the radioactivity was eluted as a broad peak surrounding the fractions containing unlabeled $ACTH_{1-24}$ (panel Ab). No radioactive material emerged at low ionic strength and pH (panel Aa). After hydrolysis, the situation was reversed (panels Ba and Bb): the radioactivity was no longer associated with $ACTH_{1-24}$ (E) and other polycationic peptides (D) but appeared at lower pH and ionic strength. Thus, 92% of the total radioactivity was found in the fractions containing the small peptides (A–C) derived from the N-terminal nonapeptide segment of $ACTH_{1-24}$. Only 8% of the total radioactivity appeared in the polycation fractions D and E.

Because of the very low labeling rate (one atom of ^{125}I in about 25 000 molecules of $ACTH_{1-24}$), it appeared rather improbable that one peptide molecule would carry more than one 1-(trifluoromethyl)-1-(3-[^{125}I]iodophenyl)methyl substituent. If the substitution had occurred at aromatic or aliphatic side chains only, the cationic properties and, thus, the chromatographic behavior in our system would not have been

influenced. However, substitution at basic groups (amino, guanido, imidazole) would have been expected to reduce the pK values of such functional groups to some extent and to change slightly the peptide elution volumes. This makes it difficult to assign structures to the small labeled peptides. It is highly probable that the radioactive peaks emerging with peptides A and B actually represent derivatives of SMEHF and SY, respectively. On the other hand, it was impossible that they (and the intermediate peaks) represented derivatives of polycationic species.

We therefore conclude that, in the presence of PC–PA (9:1) vesicles, $ACTH_{1-24}$ was labeled by [^{125}I]TID mainly through its N-terminal nonapeptide segment, whereas the C-terminal region, amino acids 10–24, remained practically unlabeled.

(6) Edman Degradation of $ACTH_{1-24}$ Labeled with [^{125}I]TID in the Presence of PC–PA (9:1) Vesicles. During Edman degradation, about 60% of the radioactive material introduced into the cup was not degraded. Of the 40% appearing in the phenylthiohydantoin fractions, strong labeling was associated with the cycles releasing Tyr^2, His^6, Phe^7, and Trp^9. Very low amounts of radioactivity were released in the cycles degrading the C-terminal segment from Pro^{12} to Tyr^{23}.

Edman degradation of peptides labeled with [^{125}I]TID could have started easily only with those molecules containing a free N-terminal amino acid residue, as a substitution with the 1-(trifluoromethyl)-1-(3-[^{125}I]iodophenyl)methyl group was expected to reduce the reactivity of amino groups toward phenylisothiocyanate quite considerably. Thus, the degradation, once started, could have only proceeded readily until a labeled peptide bond was reached, where it would have been retarded. Labeling of the N-terminal α-amino group was quite probable (Brunner & Semenza, 1981) and may explain the 40% of degradation observed here. Indeed, the material remaining in the aqueous phase of the cup had the same elution volume as $ACTH_{1-24}$ upon chromatography over Sephadex G-50 and was also hydrolyzed by pepsin. Thus, the labeling rate of the individual amino acids was certainly underestimated by the Edman procedure. Furthermore, if peptide bonds in the chain were also substituted, the underestimation would have tended to increase toward the C terminus.

The relative rates of labeling were high for aromatic amino acids and histidine and lower for aliphatic amino acids, as expected from their relative nucleophilicity and electron-donor properties (Brunner & Richards, 1980). From the results of the Edman degradation alone, it would have been impossible to decide whether or not the decreased labeling rate of Tyr^{23} (in comparison to that of Tyr^2) was to be explained by increasing underestimation toward the C terminus or by decreased vesicle-mediated contact with the photolabel.

However, in spite of all these uncertainties, the results of the Edman degradation were remarkably consistent with those obtained by chymotryptic hydrolysis. We therefore concluded that vesicle-mediated hydrophobic labeling affected mainly the N-terminal nonapeptide or undecapeptide segments of $ACTH_{1-24}$ and left the remaining C-terminal segment practically unlabeled.

(7) Vesicle Surface Charge Density and Hydrophobic Labeling of $ACTH_{1-24}$. If the labeling of $ACTH_{1-24}$ actually occurred through direct contacts with the [^{125}I]TID dissolved in the lipid vesicle membranes, then an increase of the peptide concentration on the vesicle surface should lead to a corresponding increase of the labeling rate. This was checked by variation of the bulk peptide concentration (section 8) and by variation of the electrostatic interaction. For this purpose, a fixed concentration of $ACTH_{1-24}$ was labeled in the presence

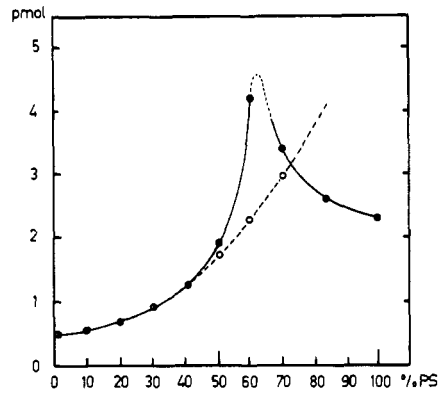

FIGURE 4: Hydrophobic labeling of $ACTH_{1-24}$ as a function of liposome composition. (Abscissa) PC–PS variation from 100% PC to 100% PS. (Ordinate) Labeling rate, P_i, expressed as amount of peptide labeled. (●) Measured P_i; (○) relative rates for electrostatic interactions only calculated according to eq 1 on the empirical basis of P_i = 0.85 pmol at 30% PS.

of liposomes containing different ratios of zwitterionic to anionic lipids (Figure 4). On going from pure PC to pure PS vesicles, an 8-fold increase of the labeling rate was observed between 0% and 62% anionic lipid. This was followed by a sharp decrease to about half of the peak value at 100% phosphatidylserine.

According to the Gouy–Chapman theory, the surface concentration, $c_i(0)$, of a given ionic species is proportional to the square of the surface charge density, σ, if all other parameters are kept constant. If we expect the labeling rate of the peptide, P_i, to be proportional to its surface concentration, then it should also be proportional to the square of the molar percentage, Q, of phosphatidylserine in the vesicles:

$$P_i \propto c_i(0) \propto \sigma^2 \propto Q^2 \qquad (1)$$

As can be seen from Figure 4, this was the case up to Q about 0.4–0.5. A strong increase above the calculated values between Q = 0.5 and 0.6 may reflect a deviation from the Gouy–Chapman theory caused by an inhomogeneous distribution of the surface potential due to the adsorption of the positively charged $ACTH_{1-24}$ molecules in discrete positions on the surface (Schoch & Sargent, 1980). However, this remains to be proved.

The sharp decrease of P_i above Q = 0.62 was perhaps caused by instability of the liposomes due to their high surface charge density.

We concluded that the increase of the labeling rate with the square of the surface charge density up to Q = 0.4–0.5 was strong evidence that the interaction between the peptide and the liposome surface was the main source of $ACTH_{1-24}$ labeling (vesicle-mediated hydrophobic labeling).

(8) Concentration Dependence of Hydrophobic Labeling of $ACTH_{1-24}$ with Negatively Charged and Neutral Vesicles. Neutralization of the positive charges of $ACTH_{1-24}$ molecules on the negatively charged surface of the PC–PA or PC–PS vesicles could, in principle, cause an aggregation of the peptide on the vesicle surface. The photolabel could then partition into the hydrophobic regions (mainly the N-terminal segments) of the peptide aggregates and thus label $ACTH_{1-24}$ upon illumination. Such a neutralization mechanism would be impossible on the surface of neutral vesicles.

In order to examine this problem, the dependence of hydrophobic labeling on peptide concentration was investigated for anionic and for neutral vesicles. As shown in Figure 5, the labeling proceeded in a saturable manner. The shape of the log dose/labeling rate curves was the same in both cases.

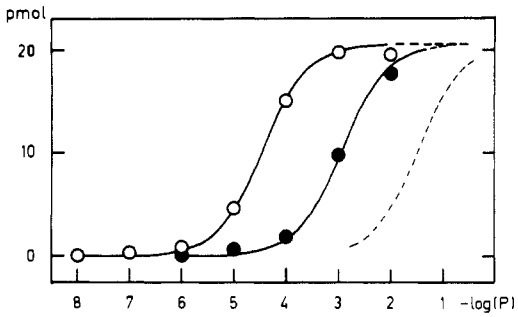

FIGURE 5: Vesicle-mediated hydrophobic labeling of $ACTH_{1-24}$ with 2×10^5 Bq of [^{125}I]TID as a function of peptide concentration. (Abscissa) Negative decadic logarithm of peptide molarity. (Ordinate) Amount of $ACTH_{1-24}$ labeled in the presence of PC–PA (9:1) vesicles (○) and of PC vesicles (●) composed of 1.5 mg of lipid; volume 1 mL of buffer A; blank values subtracted. (Dashed line) Labeling of PC vesicles expected for Boltzman distribution.

With neutral vesicles, EC_{50} was about 1 mM, with anionic vesicles about 30 μM. Saturation was explained by the limited amount of [^{125}I]TID that was identical in each experiment.

The shift of EC_{50} to about 30 times higher $ACTH_{1-24}$ concentrations on going from negatively charged to neutral vesicles was expected to be larger: according to the Boltzman distribution alone, it should have amounted to about 1000-fold (Gremlich et al., 1981). Thus, $ACTH_{1-24}$ was unexpectedly strongly labeled in the presence of neutral vesicles. This excluded surface aggregation by charge neutralization as the sole cause of labeling and was a strong indication for labeling through hydrophobic interactions between $ACTH_{1-24}$ and the lipid vesicle membranes. This interpretation was in complete agreement with the spectroscopic findings of Gremlich et al. (1983), which clearly show that $ACTH_{1-24}$ (in contrast to $ACTH_{1-10}$ or $ACTH_{11-24}$) is adsorbed to neutral membranes and that the specific conformation transitions connected with the adsorption are more pronounced at lower ratios of peptide to lipid than at higher ones. We therefore concluded that vesicle-mediated hydrophobic labeling of $ACTH_{1-24}$ was caused by hydrophobic contacts between the peptide and the membranes.

(*9*) *Equilibrium Dialysis of $ACTH_{1-24}$ and $ACTH_{11-24}$ against Lipid Vesicles.* Using $ACTH_{1-24}$ labeled with ^{125}I as a tracer, the interactions of $ACTH_{1-24}$ and $ACTH_{11-24}$ with anionic and neutral vesicles were examined by equilibrium dialysis. The results are displayed in Figure 6. $ACTH_{1-24}$ was concentrated in the anionic vesicle compartment in a saturable manner with an apparent dissociation constant K' = 16 μM, which is in good agreement with EC_{50} = 30 μM found in the labeling studies (section 8). Addition of 1 mM $ACTH_{11-24}$ competitively inhibited the process, resulting in a K'' = 0.26 mM. In concentrations up to 1 mM, $ACTH_{1-24}$ was, with this method, not found to be accumulated in the compartment containing neutral vesicles.

The results were explained by electrostatic interaction of the polycations, $ACTH_{1-24}$ (6+) and $ACTH_{11-24}$ (6+), with the negatively charged vesicle surfaces. Although interactions with neutral vesicles had been demonstrated with hydrophobic labeling (Figure 5), no such an interaction was detected by equilibrium dialysis. This was almost certainly due to the large difference between the detection limits of the two methods: they were about 0.1 pmol (labeling) and 1 μmol (equilibrium dialysis)), respectively.

Application of the Gouy–Chapman and the Boltzman equations showed that, at a bulk concentration of 10 μM $ACTH_{1-24}$ in buffer A, the calculated surface potential was V_e = 45 mV and the calculated surface concentration of

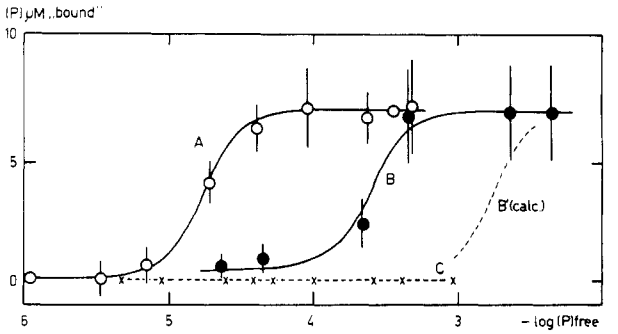

FIGURE 6: Equilibrium dialysis of $ACTH_{1-24}$ against PC–PA (9:1) vesicles in the absence (A) and in the presence (B) of 1 mM $ACTH_{11-24}$ and against neutral PC vesicles (C).

$ACTH_{1-24}$ was c_0 ($ACTH_{1-24}$) = 0.37 M. The same surface concentration, c_0 ($ACTH_{1-24}$) = 0.36 M (at V_e = 25 mV), was calculated for 1 mM $ACTH_{1-24}$ in the presence of 1 mM $ACTH_{11-24}$. Thus, taking into account only the electrostatic interactions between the anionic vesicles and $ACTH_{1-24}$ or $ACTH_{11-24}$, we would have expected the two curves A and B of Figure 6 to be separated by a factor of 100. The observed factor, however, was only 16. Such a reduction could be explained either by an abnormally weak electrostatic interaction of $ACTH_{11-24}$ (6+) with the vesicles or by an exceptionally strong vesicle interaction of $ACTH_{1-24}$. We found no plausible explanation for an abnormally weak interaction of $ACTH_{11-24}$. However, in $ACTH_{1-24}$, the segment 1–10 could have contributed an additional hydrophobic interaction to the electrostatic interaction of the segment 11–24. We therefore concluded that the discrepancies between the observed and calculated differences in the concentration dependence of vesicle-mediated labeling (section 8) and in equilibrium dialysis studies were most probably caused by hydrophobic $ACTH_{1-24}$ vesicle interactions that were largely missing in $ACTH_{1-10}$ and $ACTH_{11-24}$. This view was supported by the spectroscopic observations of Gremlich et al. (1983).

Conclusions and Projections

(1) If judiciously applied, vesicle-mediated hydrophobic photolabeling with the reagent of Brunner & Semenza (1981) can be used to characterize hydrophobic contacts of peptides with artificial lipid vesicles on a molecular level.

(2) The general position of the label within $ACTH_{1-24}$ can be assessed by proteolytic hydrolysis of the labeled peptide. Edman degradation is less reliable but can be used to check the results obtained by other methods. Detailed chemical investigations of labeled peptides and amino acids are necessary for further progress in the application of the method.

(3) The message segment of ACTH, $ACTH_{1-10}$ (net charge 0), forms aggregates with the hydrophobic photolabel in aqueous solution, probably reflecting self-aggregation. However, despite its hydrophobic character, it reacts only negligibly with neutral and anionic liposomes.

(4) The address segment, $ACTH_{11-24}$ (6+), interacts electrostatically with anionic liposomes as shown by equilibrium dialysis experiments in which it displaces [^{125}I]iodo-$ACTH_{1-24}$ (6+) from the vesicle compartment. Despite this interaction and the presence of hydrophobic amino acid side chains, it is not subject to vesicle-mediated hydrophobic photolabeling.

(5) The biologically active peptide, $ACTH_{1-24}$ (6+), interacts hydrophobically with neutral liposomes and hydrophobically plus electrostatically with anionic vesicles. As expected, its address segment, residues 11–24, remains unlabeled in both cases. However, its message segment, residues

1–10, is distinctly labeled, showing that this segment is responsible for the hydrophobic vesicle interaction of $ACTH_{1-24}$.

(6) The message segment can enter into the membrane only if it is covalently attached to the address segment. In this respect, $ACTH_{1-24}$ resembles $dynorphin_{1-13}$ (Gysin & Schwyzer, 1983b). This conclusion is supported by the spectroscopic experiments of Gremlich et al. (1983) showing that the message of $ACTH_{1-24}$ penetrates perpendicularly into the hydrophobic layer of planar phosphatidylcholine membranes only when attached to the address, which remains in the aqueous membrane interface.

(7) Relatively strong hydrophobicity is an insufficient condition for causing hydrophobic membrane contacts of the message peptides $ACTH_{1-10}$ and $dynorphin_{1-4}$. The presence of the address segments, $ACTH_{11-24}$ and $dynorphin_{5-13}$, produces amphiphilic peptides that can interact specifically with lipid membranes.

(8) The amphiphilicity of $ACTH_{1-24}$ and $dynorphin_{1-13}$ arises from the segmental arrangement of hydrophilic and hydrophobic amino acid residues into a predominantly hydrophilic (address) and a predominantly hydrophobic (message) sequence. This (new) type of amphiphilic peptide structure may be called a primary amphiphilic structure (primary amphiphilicity). The primary amphiphilic structure contrasts to the secondary amphiphilic structures (secondary amphiphilicity) caused by secondary folding of chains into amphiphilic helixes [for a recent review, see Kaiser & Kézdi (1983)] or amphiphilic β-structures.

(9) The segregation of hydrophilic and hydrophobic residues and their segmental arrangement in the primary amphiphilic structures corresponds to the sychnologic arrangement of biologically significant amino acid residues of flexible peptides into discrete segments as derived from structure–function relationships (Schwyzer, 1977).

The interdispersion of hydrophobic and hydrophilic residues necessary for producing amphiphilic secondary structures corresponds to the pharmacologically defined "rhegnylogic" arrangement of amino acid residues in peptide (or protein) agonists that rely on a (preformed) preferred secondary structure for their biologic activity (Schwyzer, 1977).

(10) Quantitative relationships between the agonistic and inhibitory potencies of ACTH peptides and their membrane interactions have been established (Gysin & Schwyzer, 1983a). This indicates that some peptides may actually depend on specific membrane interactions for their biological actions. In considering quantitative structure–activity relationships of peptides a new structural parameter (besides overall lipophilicity) must be introduced, namely, amphiphilicity, which perhaps will have to be measured through membrane interactions.

(11) The view of a receptor protein exposing its recognition site (discrimator site) toward the aqueous layer of the target cell membrane may have to be revised in some instances. The recognition of anisotropic, hydrophobic peptide–membrane interactions reveals the possibility that such sites remain buried in the hydrocarbon or hydrogen belt layers of the membrane and are actually not exposed to water.

(12) ACTH target cells contain roughly the same ratio of anionic to neutral lipids (Seltzmann et al., 1974) as our PC–PA (9:1) liposomes. At a maximal occupation of neutral membranes, $ACTH_{1-24}$ interacts with lipid patches containing about 100–200 lipid molecules (Gremlich et al., 1981, 1983). On anionic membranes, the patches may be considerably smaller. The surface area of the large, neutral patches ($\sim$10–20 nm^2) is of the same order of magnitude as the area that may be covered by a complex receptor organized in the same manner as an immunoglobulin [$\sim$10–20 nm^2 (see Metzler (1977))]. On the assumption that the cell surface area occupied by receptors is a small fraction [$\sim$0.1% (Berg & Purcell, 1977)] of that covered by lipid, then the number of receptors will be $^1/_{1000}$ of the number of patches on neutral vesicles or even less on anionic vesicles. Thus, with $K' \simeq 20\ \mu M$ for PC–PA (9:1) liposomes, a number of $ACTH_{1-24}$ molecules equal to $^1/_2$ the number of receptor molecules will be present in the lipid phase at nanomolar bulk concentrations of the hormone. This is clearly within the EC_{50} range observed with pharmacological and binding studies (Schwyzer, 1977). The number of agonist molecules in the membrane should, because of a rapid two-dimensional receptor search, suffice for the occupation of a considerable fraction of the receptor population via membrane interaction alone. However, this simplistic view may not apply to living biomembranes, because it neglects the contributions of specific lipids and proteins to the interaction. This problem remains to be studied with membranes prepared from target cells.

Registry No. $ACTH_{1-10}$, 2791-05-1; $ACTH_{11-24}$, 4237-93-8; $ACTH_{1-24}$, 16960-16-0.

References

Adam, G., & Delbrück, M. (1968) in *Structural Chemistry and Molecular Biology* (Rich, A., & Davidson, N., Eds.) pp 198–215, Freeman, San Francisco.

Berg, H. C., & Purcell, E. M. (1977) *Biophys. J. 20*, 193–219.

Brunner, J., & Richards, F. M. (1980) *J. Biol. Chem. 255*, 3319–3329.

Brunner, J., & Semenza, G. (1981) *Biochemistry 20*, 7174–7182.

Eberle, A. N., & Hübscher, W. (1979) *Helv. Chim. Acta 62*, 2460–2483.

Enoch, H. G., & Strittmatter, P. (1979) *Proc. Natl. Acad. Sci. U.S.A. 76*, 145–149.

Frank, G., & Zuber, H. (1976) *Hoppe-Seyler's Z. Physiol. Chem. 357*, 585–592.

Gremlich, H.-U., Sargent, D. F., & Schwyzer, R. (1981) *Biophys. Struct. Mech. 8*, 61–65.

Gremlich, H.-U., Fringeli, U.-P., & Schwyzer, R. (1983) *Biochemistry 22*, 4257–4263.

Gysin, B., & Schwyzer, R. (1983a) *FEBS Lett. 158*, 12–16.

Gysin, B., & Schwyzer, R. (1983b) *Arch. Biochem. Biophys. 225*, 467–474.

Kaiser, E. T., & Kézdi, F. G. (1983) *Proc. Natl. Acad. Sci. U.S.A. 80*, 1137–1143.

Kato, T., & Sasaki, M. (1975) *Anal. Biochem. 66*, 515–522.

Klein, R. (1970) *Biochim. Biophys. Acta 210*, 483–486.

Meister, N., & Müller, M. (1980) *Electron Microsc. 2*, 742–743.

Metzler, D. E. (1977) *Biochemistry, The Chemical Reactions of Living Cells*, pp 285–287, Academic Press, New York.

Müller, M., Marti, T., & Kriz, S. (1980) *Electron Microsc. 2*, 720–721.

Rae, P. A., & Schimmer, B. P. (1974) *J. Biol. Chem. 249*, 5649–5653.

Raheja, R. K., Kaur, C., Singh, A., & Bhalia, I. S. (1973) *J. Lipid Res. 14*, 695–697.

Reisfeld, R. A., Lewis, U. J., & Williams, D. E. (1962) *Nature (London) 195*, 281–283.

Schoch, P., & Sargent, D. F. (1980) *Biochim. Biophys. Acta 602*, 234–247.

Schulster, D., & Schwyzer, R. (1980) in *Cellular Receptors for Hormones and Neurotransmitters* (Schulster, D., & Levitzki, A., Eds.) pp 197–207, Wiley, New York.

Schwyzer, R. (1963) *Pure Appl. Chem. 6*, 265–295.
Schwyzer, R. (1977) *Ann. N.Y. Acad. Sci. 297*, 3–26.
Schwyzer, R., & Kappeler, H. (1963) *Helv. Chim. Acta 46*, 1550–1572.
Schwyzer, R., Gremlich, H.-U., Gysin, B., & Fringeli, U.-P. (1983) in *Peptides 1972* (Bláha, K., & Maloň, P., Eds.) pp 55–71, de Gruyter, Berlin and New York.
Shepherd, R. G., Wilson, S. D., Howard, K. S., Bell, P. H., Davis, D. S., Eigner, E. A., & Shakespeare, N. E. (1956) *J. Am. Chem. Soc. 78*, 5067–5076.
Singleton, W. S., Gray, M. S., Brown, M. L., & White, J. L. (1956) *J. Am. Chem. Soc. 42*, 53–56.
Sonenberg, M., & Schneider, A. S. (1977) *Recept. Recognition, Ser. A 4*, 1–73.
Tarr, G. E., Beecher, J. F., Bell, M., & McKean, D. J. (1978) *Anal. Biochem. 84*, 622–627.

Proflavin Binding within the Fibrinopeptide Groove Adjacent to the Catalytic Site of Human α-Thrombin†

Steven A. Sonder and John W. Fenton II*

ABSTRACT: Human α-thrombin with high fibrinogen-clotting activity binds proflavin at a single specific site (n = 0.996 site/α-thrombin, K_d = 22.0 μM) with the same affinity as the bovine enzyme (K_d = 22 ± 3 vs. 24 ± 3 μM, respectively, at pH 7.4, ~23 °C). This human enzyme form further displayed no significant difference in its ability to bind the dye over a broad NaCl concentration range (0.15–3 μM), and its hydrolysis of Bz-Arg-OEt was inhibited by the dye in a simple competitive manner (K_i = 30 ± 3 μM). Conversion of the human α- to γ-thrombin by controlled tryptic digestion essentially destroyed clotting activity without appreciably altering synthetic substrate activities and caused only ~2-fold reduction in proflavin binding. Chemical modification of approximately four tryptophans or approximately four tyrosines per enzyme also caused analogous differential losses of clotting vs. synthetic substrate activities and reduced proflavin binding ~5- and ~10-fold, respectively. Inactivation of the enzyme by conjugation at the catalytic serine (Ser-195, chymotrypsin numbering) with $MeSO_2$-F, $PhMeSO_2$-F, or i-Pr_2P-F decreased binding ~4-, 26-, and 55-fold, respectively, following the increasing size and steric hindrance properties of the conjugated group. Conjugation of the catalytic histidine (His-57) with Tos-Lys-CH_2-Cl decreased binding only ~10-fold, suggesting partial displacement by the dye. Such partial displacement appeared to occur to a slightly greater extent with the conjugate of a large exo site affinity-labeling reagent, which covalently attaches to the enzyme within the fibrinopeptide groove distal to the catalytic site. On the other hand, D-Phe-Pro-Arg-CH_2-Cl, which specifically binds within the fibrinopeptide groove and covalently reacts at or adjacent to the catalytic site, reduced proflavin binding ~40-fold. These data strongly suggest that the proflavin binding site resides in an apolar active-site region, which is next to (or slightly overlaps) the catalytic site (His-57 and Ser-195) and extends into the fibrinopeptide groove. With the least sterically hindered inactivated form, $MeSO_2$-α-thrombin, hirudin displaced proflavin, while antithrombin III in the presence of heparin could not, indicating major differences in the active-site regions required for either of these protein inhibitors of α-thrombin.

Procoagulant α-thrombin has high fibrinogen clotting and all other thrombin-ascribed activities and is the central bioregulatory enzyme in hemostasis (Fenton, 1981). This serine proteinase more closely resembles the pancreatic enzyme chymotrypsin than trypsin, with respect to amino acid sequence and three-dimensional structure (Magnusson et al., 1975; Bing et al., 1981; Furie et al., 1982), although it preferentially cleaves protein substrates at arginine and secondarily at lysine bonds in a manner analogous to that of trypsin (Magnusson, 1971; Elmore, 1973). Like chymotrypsin and trypsin, α-thrombin also binds the acridine dye, proflavin, at or near its catalytic site (Koehler & Magnusson, 1974; Li et al., 1974; Berliner & Shen, 1977), while the closely related fibrinolytic enzyme, plasmin, does not bind the dye (Ryan et al., 1976). On the basis of displacement of proflavin by indole and related compounds, this dye appears to bind partially at an apolar binding site distinct from hydrophobic regions of the arginine side-chain bindng pocket (Berliner & Shen, 1977). Human γ-thrombin, which is the second autoproteolytic or tryptic derivative enzyme form, essentially lacks clotting activity yet retains most synthetic substrate activities (Fenton et al., 1977a,b). This form also binds proflavin in a manner similar to the parent α-thrombin form, suggesting that the proflavin binding site is removed from certain active-site regions required for fibrinogen recognition (Chang et al., 1979; Fenton, 1981).

The present studies were undertaken to further assess proflavin binding requirements and to localize the site in relation to the catalytic site, consisting of the His-57/Asp-102/Ser-195 triad (Figure 1). Dissociation constants (K_d)[1] were determined by spectrophotometric methods for specific proflavin binding to human and bovine α-thrombins, human γ-thrombin, chemically modified enzymatically active forms of α-thrombin with approximately four DNS-tryptophans or approximately

† From the Center for Laboratories and Research, New York State Department of Health, Albany, New York 12201. *Received June 2, 1983.* These studies were supported in part by NIH Grant HL 13160 from the National Heart, Lung, and Blood Institute and by funds from the American Heart Association, Northeastern New York Chapter (Loudonville, NY).

[1] Abbreviations: Bz-Arg-OEt, N^{α}-benzoyl-L-arginine ethyl ester; DNS-Br, dimethyl(2-hydroxy-5-nitrobenzyl)sulfonium bromide; D-Phe-Pro-Arg-CH_2-Cl, D-phenylalanyl-L-prolyl-L-arginine chloromethyl ketone; i-Pr_2P-F, diisopropyl phosphorofluoridate; K_d, dissociation constant; K_i, inhibition constant; m-CP(PBA)-F, m-[[o-[[2-chloro-5-(fluorosulfonyl)phenyl]ureido]phenoxy]butoxy]benzamidine; $MeSO_2$-F, methanesulfonyl fluoride; NO_2, nitro; NPGB, p-nitrophenyl p-guanidinobenzoate; $PhMeSO_2$-F, phenylmethanesulfonyl fluoride; SDM, standard deviation of the mean; Tos-Lys-CH_2-Cl, N^{α}-tosyl-L-lysine chloromethyl ketone; Tris, tris(hydroxymethyl)aminomethane.

0006-2960/84/0423-1818$01.50/0